



Location, stability, and reactivity of oxygen species generated by N₂O decomposition over Fe-ZSM-5 and Fe-Beta zeolites

Vladimir I. Sobolev^{a,*}, Konstantin Yu. Koltunov^{a,b}

^a Borekov Institute of Catalysis, Pr. Akademika Lavrentieva, 5, Novosibirsk 630090, Russia

^b Novosibirsk State University, Pirogova, 2, Novosibirsk 630090, Russia

ARTICLE INFO

Article history:

Received 6 May 2011

Received in revised form 4 July 2011

Accepted 7 July 2011

Available online 18 July 2011

Keywords:

N₂O decomposition

Oxygen species

Isotope exchange

Fe-ZSM-5

Fe-Beta

ABSTRACT

Reactivity of oxygen species generated by N₂O decomposition over Fe-ZSM-5 and Fe-Beta zeolites was investigated using oxygen isotopic exchange as test reaction. The generated species are very stable up to 300 °C in the absence of the organic traces or residual N₂O in the gas phase. The reactivity of the oxygen species towards organics depends on the size of the organic molecules and their ability to penetrate into the zeolite pores. For example, in case of Fe-ZSM-5 zeolite, the oxygen species react readily with toluene, but stay intact with more bulky 1,3,5-trimethylbenzene.

© 2011 Elsevier B.V. All rights reserved.

1. Introduction

N₂O decomposition over Fe-containing zeolites can be used to generate a very efficient surface oxidant. This process has been suggested to proceed over special complexes of Fe²⁺ stabilized in the micropore space of the zeolite matrix [1–22]. N₂O decomposition over the Fe²⁺ sites results in formation of reactive surface oxygen species called “α-oxygen” [23–31]. This oxygen can oxidize methane and benzene to form methanol and phenol even at room temperature [23,32–37] similar to the enzymatic catalysis by methane monooxygenase (MMO) [38,39]. The stoichiometric reactions of α-oxygen with organic substrates are very informative to elucidate the role of this species in catalytic hydroxylation. One of such catalytic reactions, oxidation of benzene to phenol with N₂O, has received considerable attention because of its potential to replace the current cumene process. Fe-ZSM-5 zeolites were shown to be excellent catalysts for this reaction giving selectivity to phenol close to 100% [40–43].

Furthermore, catalytic selective oxidation of various (substituted) aromatic compounds over ZSM-5 zeolites has been studied using nitrous oxide as oxidant. Thus, benzonitrile was oxidized to hydroxybenzonitriles with a selectivity of 73% [44]. Phenol was found to oxidize with a selectivity of 97% to dihydroxybenzenes [45]. Oxidation of toluene by N₂O led to formation of *p*-cresol with

selectivity of about 20% [46]. The comparatively low selectivity in the last case was explained by diffusion limitations for the product, which resulted in deeper oxidation. Really, diffusion inside the zeolite pores has to be kept in mind when choosing a substrate for reactions catalyzed by zeolites.

It is suggested that the majority of active sites responsible for N₂O decomposition are located inside the micropores of zeolites. Pirutko et al. [47] investigated a silylation effect on the catalytic properties of Fe-ZSM-11 in benzene oxidation by nitrous oxide. It was shown that SiO₂ deposition on the external surface of the zeolite affects practically neither the rate of benzene oxidation nor the selectivity to phenol. Ribera et al. [22] studied the oxidation of 1,3,5-trimethylbenzene with N₂O over Fe-ZSM-5 zeolite and revealed that this organic substrate is too large to fit inside the zeolite channels and thus no reaction was observed. So, when estimating the reactivity of the active oxygen species towards organic molecules, combination of two factors should be taken into account. First is a real reactivity of the oxygen species. Second is an ability of the organic molecules to reach the active oxygen.

The present work is devoted to the properties of α-oxygen generated by N₂O decomposition on two zeolite matrices with different diameter of pores, ZSM-5 and Beta zeolites. ZSM-5 has a 10-ring channels system with apertures of 0.51 nm × 0.55 nm and 0.53 nm × 0.56 nm, while Beta has 12-ring apertures of 0.66 nm × 0.67 nm and 0.56 nm × 0.56 nm [48,49]. A set of organic molecules of different size, such as toluene, *m*-xylene and 1,3,5-trimethylbenzene, was involved in the reaction with α-oxygen.

* Corresponding author. Tel.: +7 383 3269765; fax: +7 383 3308056.
E-mail address: visobo@catalysis.ru (V.I. Sobolev).

The ability of these molecules to react with active surface oxygen species was studied using O_2 isotope exchange (OIE) method.

Isotope exchange between oxygen in the gas phase and a solid oxide is a powerful tool to discriminate between oxygen species of different reactivity. In the case of Fe-containing zeolites, a significant effect of α -oxygen on the rate of O_2 exchange was shown [1,2,15,50]. Gas phase oxygen is able to exchange with surface α -oxygen even at room temperature and OIE can be used for quantitative estimation of the amount of the active surface oxygen species.

2. Experimental

Fe-ZSM-5 ($SiO_2/Al_2O_3 = 80$, 0.56 wt.% Fe) and Fe- β ($SiO_2/Al_2O_3 = 38$, 0.53 wt.% Fe) zeolites were obtained by calcination of their NH_4^+ precursors (CBV 8014 and CP 814C, respectively, from Zeolyst International) in air at 550 °C for 6 h, followed by ion exchange with 0.05 M $FeCl_3$ (4 ml per 2 g of zeolite sample) during 24 h at room temperature. The samples were washed with deionized water, and dried overnight at room temperature. Then the obtained samples were activated by calcination in air at 115 °C for 3 h and then at 550 °C for 5 h.

All adsorption and isotope exchange experiments were carried out in a vacuum static setup. The setup was made of stainless steel with a small quartz reactor and was described elsewhere [2]. The setup was equipped with an on-line mass-spectrometer (Stanford Research Systems RGA 200) to analyze the gas phase composition. The pressure of gases in the reaction volume was in the range of 0.1–2.0 Torr and was measured by Baratron capacitance manometer (MKS Instruments). A catalyst sample (0.5 g) was placed in a quartz microreactor, which can be isolated from the rest of the setup. Before each experiment the sample was pretreated in vacuum and then in oxygen at 550 °C.

The experiments included four steps that were performed in the following sequence:

- (1) α -oxygen loading;
- (2) adsorption of organic substrate over zeolite;
- (3) evacuation of the excess organic material from the gas phase;
- (4) oxygen isotope exchange.

α -Oxygen was loaded by N_2O decomposition at 250 °C as described in [1,2]. After α -oxygen deposition the reactor was isolated from the rest of the reaction volume and cooled to the experiment temperature. Gas in the reaction volume was replaced with an organic vapor which was contacted with the catalyst for 10–15 min. The excess organic material was removed by evacuation and then 0.2 Torr of labeled $^{36}O_2$ with 84% of isotope ^{18}O was introduced into the system. The exchange parameters were determined from the experimentally obtained time dependence of the isotope composition of the molecular oxygen ($^{36}O_2$, $^{34}O_2$ and $^{32}O_2$). The fraction of the ^{18}O isotope in the molecular oxygen (α) calculated as

$$\alpha = \frac{1/2 C_{34} + C_{36}}{C_{32} + C_{34} + C_{36}}$$

was used to characterize the oxygen isotope exchange. Number of exchangeable surface oxygen atoms, N_s , was calculated from the material balance:

$$\alpha^\circ * (N_g) = \alpha^\infty * (N_g + N_s)$$

$$N_s = N_g * \left(\frac{\alpha^\circ}{\alpha^\infty} - 1 \right)$$

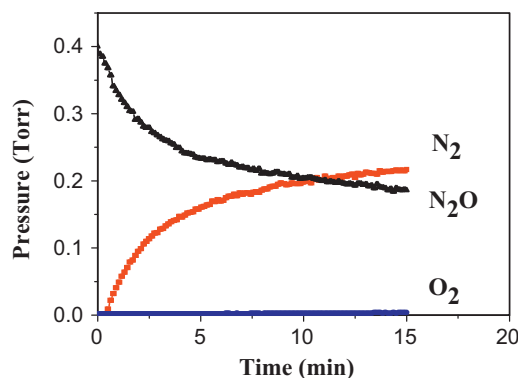


Fig. 1. N_2O decomposition over FeZSM-5 at 250 °C.

where N_g – number of oxygen atoms in the gas phase, α° and α^∞ – the initial and equilibrium values of α .

3. Results and discussion

3.1. N_2O decomposition and temperature-programmed desorption

N_2O decomposition on the Fe-ZSM-5 sample at 250 °C and N_2O initial pressure of 0.4 Torr is presented in Fig. 1. The reaction proceeds with evolution of only N_2 and formation of surface oxygen atom, $(O)_\alpha$, according to reaction (1):



These surface N_2O species are stable at 250 °C and can be removed from the surface by temperature increasing. Fig. 2 shows temperature-programmed desorption experiment after N_2O decomposition at 250 °C. Two neighboring surface $(O)_\alpha$ can recombine with evolution of molecular oxygen into the gas phase:



It is seen that desorption of O_2 begins above 315 °C, and the molecular oxygen is the only desorption product. The amount of the molecular oxygen desorbed is half of the amount of N_2O decomposed at 250 °C. So, the total amount of oxygen atoms adsorbed on the active surface sites as well as the concentration of these sites can be determined by the calculation of the amount of N_2O decomposed or the amount of O_2 desorbed in TPD experiment.

The time of N_2O decomposition shown in Fig. 1 is 15 min. After such decomposition only surface oxygen species are obtained with evolution only molecular oxygen in TPD experiment. The picture is different if time of N_2O decomposition is much longer. Fig. 3 shows

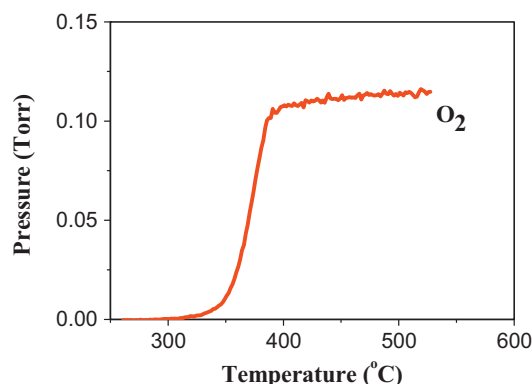


Fig. 2. TPD after N_2O decomposition for 15 min over FeZSM-5 at 250 °C.

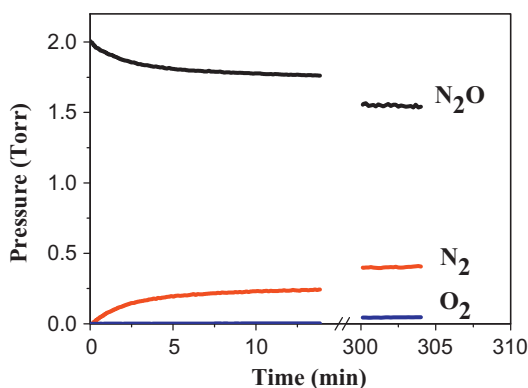


Fig. 3. N₂O decomposition over FeZSM-5 at 250 °C for 5 h.

N₂O decomposition at 250 °C within 5 h. Long-term decomposition leads to appearance of molecular oxygen in the gas phase even at 250 °C. It should be noted that after 5 h the amount of N₂ evolved into the gas phase is lower than the amount of N₂O decomposed. This fact can be explained by a parallel NO generating, which is proved by TPD experiment. Fig. 4 demonstrates O₂ and NO desorption in TPD experiment after 5-h exposure of the zeolite sample at 250 °C in 2 Torr of N₂O. Oxygen desorption begins at 290 °C, the amount of the O₂ desorbed being close to that desorbed after short-term N₂O decomposition (Fig. 2). With increase of temperature to 345 °C, NO desorption into the gas phase is observed (Fig. 4).

Formation of the surface NO during N₂O interaction with zeolite surface was observed earlier [9,51]. Bulushev et al. proposed a reaction scheme, which included two steps of N₂O decomposition [9]. The first step (fast) results in the surface α -oxygen loading on the extraframework Fe²⁺ sites. NO is formed in the second step (slow) on sites different from those for α -oxygen deposition. The formed NO leads to acceleration of surface oxygen recombination/desorption. It was shown that total amount of NO formed depends on the time of N₂O decomposition and N₂O pressure [9]. Obviously, that in the case when NO is formed, neither amount of N₂O decomposed nor amount of O₂ desorbed can be used to measure correctly the concentration of the deposited active oxygen species. In that case, only oxygen isotope exchange (OIE) method is the most suitable for the quantitative estimation of the amount of α -oxygen species.

3.2. Oxygen isotope exchange

It is well known that ¹⁸O₂ exchange activity of zeolites is negligible at temperature below 300 °C [1,2]. Preliminary N₂O decomposition with α -oxygen loading dramatically changes the

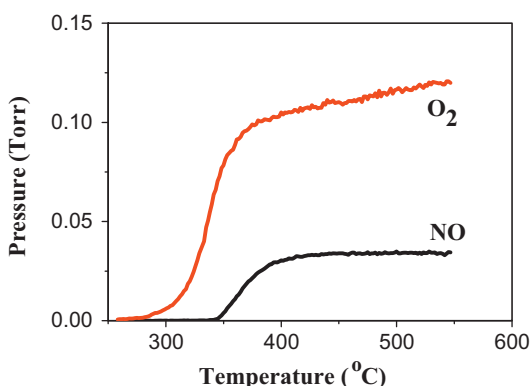


Fig. 4. TPD after N₂O decomposition for 5 h over FeZSM-5 at 250 °C.

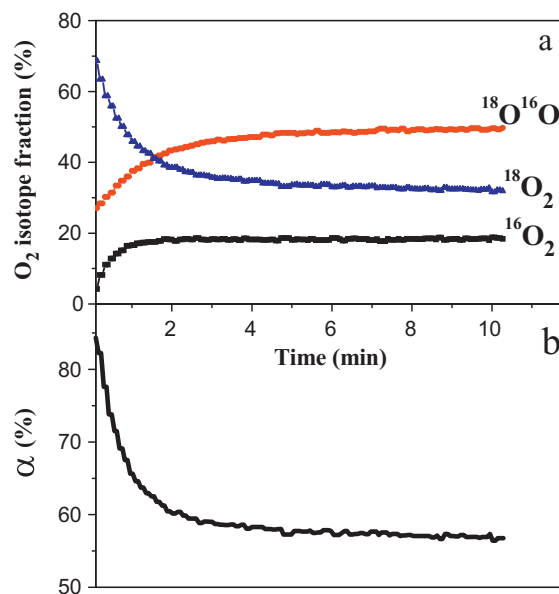


Fig. 5. Time dependence of molecular oxygen isotopic species (a) and atomic fraction ¹⁸O in the gas phase (b) during OIE experiment over FeZSM-5 at 100 °C after α -oxygen loading.

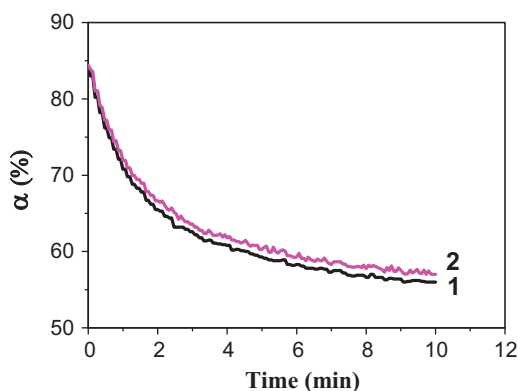
picture. Fig. 5a shows the change of O₂ isotope fractions in the gas phase at 100 °C after preliminary loading of α -oxygen on Fe-ZSM-5 zeolite at 250 °C. As appeared, it takes only 10 min to complete the isotope exchange. Fig. 5b demonstrates the change of the fraction of ¹⁸O in the gas phase oxygen, α , with time. The ¹⁸O fraction drops from the initial value of 84% to 57% for 10 min. Number of exchangeable surface oxygen atoms, N_s , calculated from isotopic material balance is found to be equal to 8.1×10^{18} oxygen atoms per gram of the catalyst (O/g).

OIE over Fe-Beta zeolite (after preliminary loading of α -oxygen at 250 °C) is similar to the exchange over Fe-ZSM-5. The number of exchangeable surface oxygen atoms calculated from the OIE experiment is equal to 8.4×10^{18} atoms O/g. The summarized results on calculation of the number of surface α -oxygen atoms derived from N₂O decomposition, temperature-programmed O₂ desorption, and O₂ isotope exchange for both Fe-ZSM-5 and Fe-Beta samples are presented in Table 1. As seen from the table, in the case of a short-term N₂O decomposition (15 min), the number of exchangeable surface oxygen atoms is close to the number of nitrous oxide molecules decomposed, as well as to the number of oxygen atoms desorbed in TPD experiments. However, for the long-term N₂O decomposition (5 h), the number of exchangeable surface oxygen atoms is less than the number of nitrous oxide molecules decomposed or the number of oxygen atoms desorbed. Obviously, this is due to the secondary reactions of the surface oxygen species with N₂O giving rise to formation and accumulation of NO molecules on the catalyst surface as was showed above. These reactions have to be taken into consideration when calculating concentration of active surface oxygen species. The method of oxygen isotope exchange is the most reliable for that.

α -Oxygen is active enough to react readily with organic molecules even at room temperature [24]. At the same time, in the absence of the organic traces (as well as inorganic reductants) in the gas phase this oxygen is very stable. Fig. 6 demonstrates such stability of α -oxygen species. Curve 1 in the figure is the time dependence of the fraction of ¹⁸O in the gas phase oxygen in the course of O₂ isotope exchange at room temperature on the Fe-Beta zeolite after preliminary N₂O decomposition. Curve 2 is the same dependence obtained after N₂O decomposition and subsequent ageing the sample for 24 h at room temperature under

Table 1The number of surface α -oxygen atoms determined from N_2O decomposition, O_2 desorption, and oxygen isotope exchange.

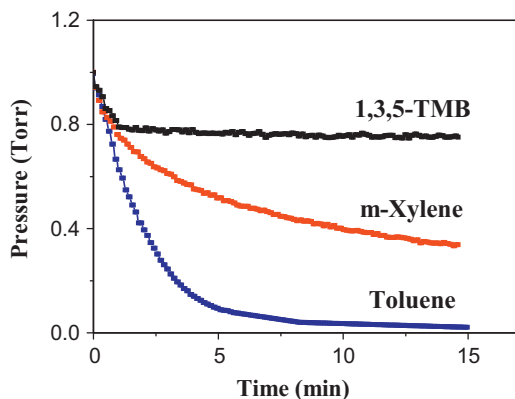
Sample	Time of N_2O decomposition (min)	Amount of N_2O decomposed (10^{18} mol N_2O/g)	Amount of O_2 desorbed in TPD (10^{18} at. O/g)	The number of exchangeable oxygen (10^{18} at. O/g)
Fe-ZSM-5	15	8.9	9.1	8.1
Fe-ZSM-5	300	19.1	11.0	7.9
Fe- β	15	9.2	8.8	8.4

**Fig. 6.** Oxygen isotope exchange over Fe- β -zeolite at 25 °C. 1 is the time dependence of the fraction of ^{18}O in the gas phase oxygen after preliminary N_2O decomposition at 250 °C. 2 is the same dependence after N_2O decomposition and keeping the sample for 24 h at 25 °C under vacuum.

vacuum. The curves came out to be very close, which means the absence of any secondary transformations of the surface α -oxygen species under the keeping at mild conditions. The stability of α -oxygen species does not depend on zeolite matrix. For Fe-ZSM-5 zeolite OIE is the same before and after the keeping the sample with α -oxygen for 24 h at room temperature. Therefore, O_2 isotope exchange can be used as indirect method to measure properly the ability of organic molecules to penetrate into zeolite micropores and react with α -oxygen.

3.3. Aromatics adsorption and reaction with α -oxygen

A set of organic aromatic molecules of different size (toluene, *m*-xylene and 1,3,5-trimethylbenzene) was used to study their reactions with α -oxygen. Initially, the adsorption of toluene, *m*-xylene and 1,3,5-TMB on Fe-ZSM-5 zeolite, pretreated with N_2O , was examined (Fig. 7). As it is seen, the adsorption strongly depends on the size of aromatic molecule. At the same initial pressure of the adsorbates, toluene is almost completely adsorbed for 10 min,

**Fig. 7.** Adsorption of toluene, *m*-xylene and 1,3,5-TMB on Fe-ZSM-5 zeolite at 100 °C after preliminary N_2O decomposition at 250 °C.

whereas only small part of 1,3,5-TMB is adsorbed for the first minute on the external surface of the zeolite without further pressure change. *m*-Xylene showed an intermediate disposition to adsorption between toluene and 1,3,5-TMB. In order to check the ability of the aromatic molecules to react with α -oxygen, O_2 isotope exchange was performed after N_2O decomposition and aromatics adsorption. The results obtained for Fe-ZSM-5 zeolite are presented in Fig. 8. Curve 1 in the figure is a blank experiment, in which O_2 isotope exchange was performed immediately after loading the surface α -oxygen without subsequent aromatic adsorption. Curve 2 corresponds to an experiment, in which isotope exchange was performed after loading the surface α -oxygen at 250 °C and subsequent 1,3,5-TMB adsorption at 100 °C. As it can be seen from the figure, the adsorption of 1,3,5-TMB weakly influences the intensity of OIE, which is very close to that in the blank experiment. This indicates that no penetration of this bulky (for ZSM-5) molecule occurs or such penetration is very negligible. In contrast, toluene molecules definitely penetrate into ZSM-5 channels since no O_2 isotope exchange is observed due to total α -oxygen consumption (Fig. 8; Curve 4). The adsorption of *m*-xylene, which leads only to partial α -oxygen consumption, may be considered as an intermediate case (Fig. 8; Curve 3).

The ability of bulky molecules to penetrate into zeolite pores depends on temperature: Fig. 9 shows OIE on Fe-ZSM-5 after α -oxygen loading (1) and subsequent adsorption of *m*-xylene at 25 °C (2), 100 °C (3), and 195 °C (4). Usually the oxygen isotope exchange experiments were performed at 100 °C. The only exception was OIE after adsorption of *m*-xylene at 25 °C. The same temperature (25 °C) was chosen for OIE in order to avoid an additional penetration of the adsorbed (on the external surface) *m*-xylene into zeolite pores, which could lead to erroneous results.

The higher the temperature of *m*-xylene adsorption, the higher amount of α -oxygen consumed in the reaction with *m*-xylene. Indeed, almost all the loaded α -oxygen is reacted with *m*-xylene adsorbed at 195 °C and the following OIE is practically not observed (Fig. 9; Curve 4). The calculated data on the residual and consumed α -oxygen are summarized in Table 2.

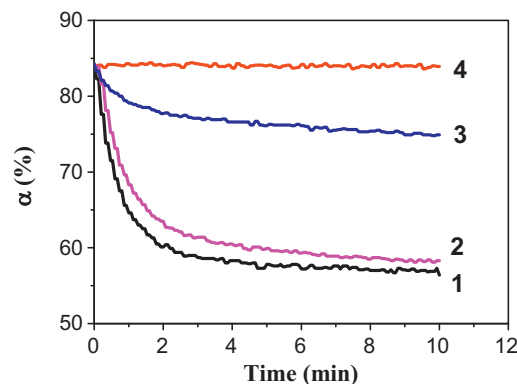
**Fig. 8.** Oxygen isotope exchange over FeZSM-5 at 100 °C after α -oxygen loading (1), α -oxygen loading and adsorption of 1,3,5-TMB (2), *m*-xylene (3), toluene (4) at 100 °C.

Table 2
The effect of organic substrate adsorption on consumption of α -oxygen in the FeZSM-5 zeolite.

Substrate	Adsorption temperature ($^{\circ}$ C)	Content of α -oxygen (10^{18} at. O/g)	Fraction of α -oxygen reacted (%)
–	–	8.1	0
Toluene	100	0	100
<i>m</i> -Xylene	25	5.8	28
<i>m</i> -Xylene	100	2.5	69
<i>m</i> -Xylene	195	0.3	96
1,3,5-TMB	100	7.9	2

The conformity of the molecular size with the pore diameter of zeolite is essential to understanding the ability of the molecules to penetrate into zeolite microporous space and to react with α -oxygen. ZSM-5 has a 10-ring channels system with apertures of $0.51 \text{ nm} \times 0.55 \text{ nm}$ and $0.53 \text{ nm} \times 0.56 \text{ nm}$, while Beta has 12-ring apertures of $0.66 \text{ nm} \times 0.67 \text{ nm}$ and $0.56 \text{ nm} \times 0.56 \text{ nm}$, as measured by X-ray diffraction [48,49]. The accuracy of these values has been disputed because organic molecules that are larger than a reported XRD zeolite pore diameters can adsorb and diffuse through the pores. Many authors ascribe this discrepancy between reported crystallographic pore sizes of zeolites and molecular sizes of the reacted molecules to thermal vibrations as well as the distortion of the crystal lattice of zeolite and the adsorbed molecules.

Webster et al. have considered the concept of temperature dependent *effective catalytic pore size* of zeolites [52]. They calculated the effective pore size for HZSM-5 as a function of temperature and concluded that at 300°C the size is between 0.662 and 0.727 nm and is increased to a minimum of 0.764 nm at 370°C . The concept of *effective minimum molecular dimensions* has been set forth by the same authors [53]. According to Webster a molecule can enter a cylindrical pore if the minimum dimension of the molecule (MIN-1) and the second minimum dimension (MIN-2) are equal to or smaller than the pore diameter. The values MIN-1 and MIN-2 calculated by Webster were 0.401 and 0.663 nm (for toluene), 0.395 and 0.726 nm (for *m*-xylene), 0.406 and 0.818 nm (for 1,3,5-TMB) [53].

The similar results for adsorption of toluene, *m*-xylene, 1,3,5-trimethylbenzene and their reactions with α -oxygen were obtained in a case of Fe- β -zeolite. It has 12-ring apertures of $0.66 \text{ nm} \times 0.67 \text{ nm}$ and $0.56 \text{ nm} \times 0.56 \text{ nm}$, which are larger than 10-ring apertures of ZSM-5 zeolite. So, it can be expected that adsorption of organic substrates and their reaction with surface α -oxygen will be favored for the β -zeolite. Fig. 10 shows OIE after N_2O decomposition and aromatics adsorption for the Fe- β -zeolite. Curve 1 corresponds to a blank experiment, in which OIE was performed just after the loading of surface α -oxygen. Curve 2 is an experiment where isotope exchange was performed after the load-

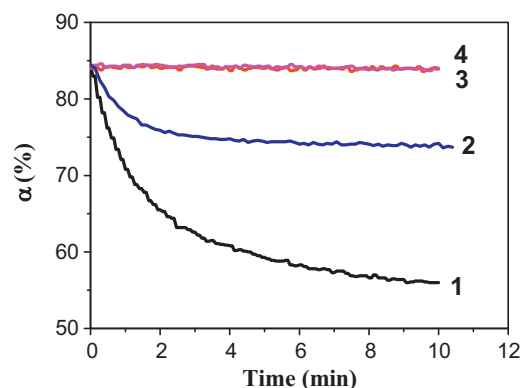


Fig. 10. Oxygen isotope exchange over Fe- β -zeolite at 100°C after α -oxygen loading (1), α -oxygen loading and adsorption of 1,3,5-TMB (2), *m*-xylene (3), toluene (4) at 100°C .

ing of α -oxygen followed by 1,3,5-TMB adsorption at 100°C . As it can be seen, a part of α -oxygen is reacted with 1,3,5-TMB and therefore it does not participate in the exchange. Curves 3 and 4, obtained for OIE after α -oxygen loading and subsequent adsorption of *m*-xylene and toluene, are practically coincident. Since no O_2 isotope exchange was observed (due to total α -oxygen consumption) it can be concluded that *m*-xylene and toluene molecules penetrate easily into the β -zeolite channels.

Monitoring of OIE after N_2O decomposition and following organics adsorption allows studying kinetics of organic molecules penetration into zeolite channels. Fig. 11 demonstrates an effect of 1,3,5-TMB adsorption time on O_2 isotope exchange. As expected, no significant difference with a blank experiment (1) was observed in the case of α -oxygen loading followed by a 24 h ageing in vacuum (2). Only adsorption of 1,3,5-TMB leads to decrease of the amount of α -oxygen participating in the exchange. The increasing time of 1,3,5-TMB adsorption from 1.5 h to 24 h results in the increasing the amount of α -oxygen reacted with 1,3,5-TMB and the decreasing the amount of α -oxygen free for the oxygen isotope

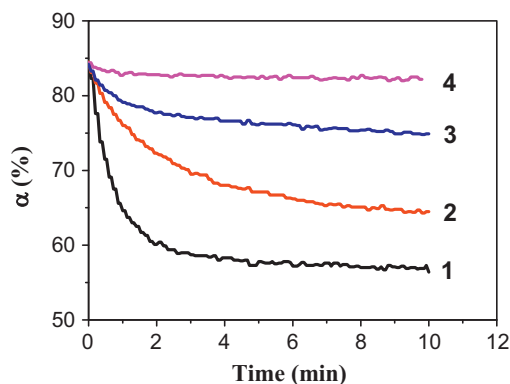


Fig. 9. Oxygen isotope exchange over FeZSM-5 at 100°C : after α -oxygen loading (1); α -oxygen loading and adsorption of *m*-xylene at 25°C (2) (the exchange is also performed at 25°C), 100°C (3), and 195°C (4).

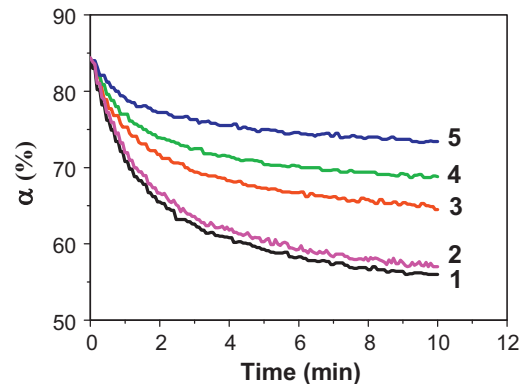


Fig. 11. Oxygen isotope exchange over Fe- β -zeolite at 20°C after α -oxygen loading (1), α -oxygen loading followed by a 24 h ageing at 25°C in vacuum (2), α -oxygen loading and adsorption of 1,3,5-TMB at 25°C for 1.5 h (3), 4.5 h (4), and 24 h (5).

Table 3The effect of organic substrate adsorption on consumption of α -oxygen in the Fe- β -zeolite.

Substrate	Adsorption temperature (°C)	Time of exposure	Content of α -oxygen (10^{18} at. O/g)	Fraction of α -oxygen reacted (%)
–	–	–	8.4	0
Toluene	100	10 min	0	100
<i>m</i> -Xylene	100	10 min	0	100
1,3,5-TMB	100	10 min	2.3	73
1,3,5-TMB	20	1.5 h	5.2	38
1,3,5-TMB	20	4.5 h	3.8	55
1,3,5-TMB	20	24 h	2.6	69

exchange. The quantitative data on the residual and consumed α -oxygen after adsorption of the organic substrates on Fe- β -zeolite are summarized in Table 3.

4. Conclusions

Reactions of α -oxygen species generated by N_2O decomposition over Fe-ZSM-5 and Fe-Beta zeolites with various methylbenzenes (toluene, *m*-xylene and 1,3,5-trimethylbenzene) are studied. For these organic molecules the ability to react with α -oxygen strongly depends on the conformity of the molecule size with the pore diameter of the zeolite, which supports a viewpoint on α -oxygen species location mainly inside the micropores of zeolites. For Fe-ZSM-5 zeolite, toluene molecules can easily penetrate into channels and react with α -oxygen. However, 1,3,5-trimethylbenzene molecules are too bulky to penetrate into ZSM-5 channels, so α -oxygen generated on Fe-ZSM-5 stay intact. For Fe- β zeolite, slow diffusion of 1,3,5-trimethylbenzene into channels and its reaction with α -oxygen is disclosed.

References

- [1] G.I. Panov, V.I. Sobolev, A.S. Kharitonov, J. Mol. Catal. 61 (1990) 85–97.
- [2] V.I. Sobolev, G.I. Panov, A.S. Kharitonov, V.N. Romannikov, A.M. Volodin, K.G. Ione, J. Catal. 139 (1993) 435–443.
- [3] V.I. Sobolev, G.I. Panov, A.S. Kharitonov, V.N. Romannikov, A.M. Volodin, Kinet. Catal. 34 (1993) 797–802.
- [4] A.M. Volodin, V.I. Sobolev, G.M. Zhidomirov, Kinet. Catal. 39 (1998) 775–787.
- [5] E.J.M. Hensen, Q. Zhu, M.M.R.M. Hendrix, A.R. Overweg, P.J. Kooyman, M.V. Sychev, R.A. van Santen, J. Catal. 221 (2004) 560–574.
- [6] E.J.M. Hensen, Q. Zhu, R.A. van Santen, J. Catal. 220 (2003) 260–264.
- [7] E.J.M. Hensen, Q. Zhu, R.A.J. Janssen, P.C.M.M. Magusin, P.J. Kooyman, R.A. van Santen, J. Catal. 233 (2005) 123–135.
- [8] Q. Zhu, R.M. van Teeffelen, R.A. van Santen, E.J.M. Hensen, J. Catal. 221 (2004) 575–583.
- [9] D.A. Bulushev, L. Kiwi-Minsker, A. Renken, J. Catal. 222 (2004) 389–396.
- [10] H.Y. Chen, E.M. El-Malki, X. Wang, R.A. van Santen, W.M.H. Sachtler, J. Mol. Catal. A: Chem. 162 (2000) 159–174.
- [11] E.M. El-Malki, R.A. van Santen, W.M.H. Sachtler, J. Phys. Chem. B 103 (1999) 4611–4622.
- [12] M. Hafele, A. Reitzmann, D. Roppelt, G. Emig, Appl. Catal. A: Gen. 150 (1997) 153–164.
- [13] E.J.M. Hensen, Q. Zhu, R.A. van Santen, J. Catal. 233 (2005) 136–146.
- [14] J. Jia, K.S. Pillai, W.M.H. Sachtler, J. Catal. 221 (2004) 119–126.
- [15] J. Jia, B. Wen, W.M.H. Sachtler, J. Catal. 210 (2002) 453–459.
- [16] L. Kiwi-Minsker, D.A. Bulushev, A. Renken, J. Catal. 219 (2003) 273–285.
- [17] P. Kubanek, B. Wichterlova, Z. Sobalik, J. Catal. 211 (2002) 109–118.
- [18] L.J. Lobree, I.-C. Hwang, J.A. Reimer, A.T. Bell, J. Catal. 186 (1999) 242–253.
- [19] P. Marturano, L. Drozdova, A. Kogelbauer, R. Prins, J. Catal. 192 (2000) 236–247.
- [20] J. Perez-Ramirez, F. Kapteijn, A. Bruckner, J. Catal. 218 (2003) 234–238.
- [21] J. Perez-Ramirez, G. Mul, F. Kapteijn, J.A. Moulijn, A.R. Overweg, A. Domenech, A. Ribera, I.W.C.E. Arends, J. Catal. 207 (2002) 113–126.
- [22] A. Ribera, I.W.C.E. Arends, S. de Vries, J. Peres-Ramires, R.A. Sheldon, J. Catal. 195 (2000) 287–297.
- [23] V.I. Sobolev, A.S. Kharitonov, Ye.A. Paukshtis, G.I. Panov, J. Mol. Catal. 84 (1993) 117–124.
- [24] G.I. Panov, A.K. Uriarte, M.A. Rodkin, V.I. Sobolev, Catal. Today 41 (1998) 365–385.
- [25] J. Taboada, A. Overweg, P.J. Kooyman, I.W.C.E. Arends, G. Mul, J. Catal. 231 (2005) 56–66.
- [26] E.V. Kondratenko, J. Perez-Ramirez, Appl. Catal. B 64 (2006) 35–41.
- [27] E.V. Starokon, K.A. Dubkov, L.V. Pirutko, G.I. Panov, Top. Catal. 73 (2003) 137–143.
- [28] P.K. Roy, G.D. Pirngruber, J. Catal. 227 (2004) 164–174.
- [29] I. Yuranov, D. Bulushev, A. Renken, L. Kiwi-Minsker, J. Catal. 227 (2004) 138–147.
- [30] B.R. Wood, J.A. Reimer, A. Bell, M.T. Janicke, K.C. Ott, J. Catal. 224 (2004) 148–155.
- [31] J. Novakova, Z. Sobalik, Catal. Lett. 89 (2003) 243–247.
- [32] V.I. Sobolev, K.A. Dubkov, O.V. Panna, G.I. Panov, Catal. Today 24 (1995) 251–252.
- [33] K.A. Dubkov, V.I. Sobolev, E.P. Talsi, M.A. Rodkin, N.H. Watkins, A.A. Shteinman, G.I. Panov, J. Mol. Catal. A 123 (1997) 155–161.
- [34] K.A. Dubkov, V.A. Sobolev, G.I. Panov, Kinet. Catal. 39 (1998) 72–79.
- [35] G.I. Panov, V.I. Sobolev, K.A. Dubkov, A.S. Kharitonov, Stud. Surf. Sci. Catal. 101 (1996) 493–502.
- [36] P.P. Knops-Gerrits, W.J. Smith, Stud. Surf. Sci. Catal. 130 (2000) 3531–3535.
- [37] P.P. Knops-Gerrits, W.A. Goddard III, J. Mol. Catal. 166 (2001) 135–145.
- [38] A.A. Shteinman, Russ. Chem. Bull. 50 (2001) 1795–1810.
- [39] N.S. Ovanesyan, A.A. Shteinman, K.A. Dubkov, V.I. Sobolev, G.I. Panov, Kinet. Catal. 39 (1998) 792–797.
- [40] G.I. Panov, A.S. Kharitonov, V.I. Sobolev, Appl. Catal. A: Gen. 98 (1993) 1–20.
- [41] G. Panov, CATTECH 4 (1) (2000) 18–24.
- [42] I. Yuranov, D. Bulushev, A. Renken, L. Kiwi-Minsker, Appl. Catal. A: Gen. 319 (2007) 128–139.
- [43] G. Centi, S. Perathoner, R. Arrigo, G. Giordano, A. Katovic, V. Pedula, Appl. Catal. A 307 (2006) 30–41.
- [44] H. Ehrich, W. Schwieger, K. Jahnisch, Appl. Catal. A 272 (2004) 311–319.
- [45] D.P. Ivanov, V.I. Sobolev, L.V. Pirutko, G.I. Panov, Adv. Synth. Catal. 344 (2002) 986–995.
- [46] B. Vogel, C. Schneider, E. Klemm, Catal. Lett. 79 (2002) 107–112.
- [47] L.V. Pirutko, O.O. Parenago, E.V. Lunina, A.S. Kharitonov, L.G. Okkel, G.I. Panov, React. Kinet. Catal. Lett. 52 (1994) 275–280.
- [48] Database of Zeolite Structures, <http://www.iza-structure.org/databases>.
- [49] J.B. Higgins, R.B. LaPierre, J.L. Schlenker, A.C. Rohrman, J.D. Wood, G.T. Kerr, W.J. Rohrbach, Zeolites 8 (1998) 446–452.
- [50] M.V. Parfenov, E.V. Starokon, S.V. Semikolenov, G.I. Panov, J. Catal. 263 (2009) 173–180.
- [51] L. Kiwi-Minsker, D.A. Bulushev, A. Renken, Catal. Today 110 (2005) 191–198.
- [52] C.E. Webster, R.S. Drago, M.C. Zerner, J. Phys. Chem. B 103 (1999) 1242–1249.
- [53] C.E. Webster, R.S. Drago, M.C. Zerner, J. Am. Chem. Soc. 120 (1998) 5509–5516.